*J*inst

Published by IOP Publishing for Sissa Medialab

Received: *December 7, 2023*
Accepted: *February 2, 2024*
Published: *May 17, 2024*

Light Detection In Noble Elements (LIDINE 2023)
Madrid, Spain
20–22 September 2023

Far UV coatings for liquid-Ar time projection chambers

J.I. Larruquert,[a,*] P. López-Reyes,[a] N. Gutiérrez-Luna,[a] C. Honrado-Benítez[a] and V. Pesudo[b]

[a]*GOLD, Instituto de Óptica — Consejo Superior de Investigaciones Científicas, Serrano 144, 28006, Madrid, Spain*
[b]*CIEMAT, Centro de Investigaciones Energéticas, Medioambientales y Tecnológicas, Madrid 28040, Spain*

E-mail: j.larruquert@csic.es

Abstract: Liquid Ar (LAr) and liquid Xe (LXe) time projection chambers (TPCs) are used for many applications in neutrino physics and direct dark matter searches. The performance of these detectors, particularly dual-phase ones, depends very strongly on the efficiency for detecting the far ultraviolet (FUV) scintillation light. Such detection is particularly challenging for LAr, in which the strongest scintillation feature is observed at a wavelength of 127 nm (175 nm for LXe). The current mainstream approach is covering the optical surfaces with a wavelength shifter, which absorbs de FUV light and emits at wavelengths that overlap with the optical band, where commercial devices have higher detection efficiency. This work presents coatings designed to enhance the optical properties of the detector materials and to be an alternative to the current technique. In particular, two possible coatings are proposed: narrowband and broadband FUV reflective coatings. The narrowband coatings are tuned at the FUV scintillation light. They provide a large reflectance at the design angle; additionally, these coatings are naturally transparent at longer wavelengths, which might be useful to selectively detect the wavelength of interest. Their performance is evaluated taking into account the refractive index of LAr and as a function of the angle of incidence. The same calculations are performed for an aluminium-based broadband mirror. Finally, the effect on reflectance of submerging both sorts of mirrors at liquid nitrogen temperature is presented.

Keywords: Mirror coating; Optics; Time projection Chambers (TPC)

*Corresponding author.

https://doi.org/10.1088/1748-0221/19/05/C05028

2024 JINST 19 C05028

Contents

1 Introduction

Dark Matter (DM) is a hypothetical form of matter proposed by Oort [1] and Zwicky [2, 3] in the 1930s which would make up ~85% of the total matter in the Universe [4], as indicated by many astrophysical observations [5–7]. One possible solution of the DM problem involves an extension of the Standard Model through the existence of a new elementary, massive, weakly-interacting neutral particle (WIMP). Experiments to detect WIMPs include the direct search for their interaction with ordinary matter [8–10], the search for products of annihilation [11–13] and attempts to produce them in high-energy collisions, such as in the Large Hadron Collider (LHC) [14, 15].

Current promising detectors of DM signals are dual-phase (gas-liquid) argon (Ar) or xenon (Xe) time projection chambers (TPC). These detectors aim at observing and unambiguously identifying the recoiling Ar (Xe) nucleus after a collision with a WIMP in the DM halo. This nuclear recoil moves along the liquid Ar (LAr) target and produces excited and ionized Ar atoms in its vicinity. This results in the formation of excited molecular states that, after some de-excitations, populate either singlet or triplet states [16, 17] which, in turn, decay radiatively to the unbound ground state via the emission of scintillation light. In LAr, this scintillation is centered at 127 ± 8 nm [18] in the far ultraviolet (FUV), whilst for liquid Xe (LXe) the scintillation light is produced around the 160–188 nm range [19–21]. For this light to be detected by visible sensing devices, the TPC inner surfaces are most often coated with tetraphenyl butadiene (TPB), which absorbs the 127-nm scintillation light, reemitting in the blue region (~420 nm). This procedure eliminates any chance of exploiting the spectral richness that has been a source of study in the last years [16, 22, 23].

Coatings can play an important role in minimizing the photons absorbed by the TPC walls or, alternatively, acting selectively on photons at different spectral ranges [16]. This proceeding assesses two sorts of FUV coatings: broadband mirror coatings based on Al protected with MgF_2, and narrowband mirrors based on the periodic combination of two fluorides, AlF_3/LaF_3 or MgF_2/LaF_3, that give rise to a reflectance band by interference. The coatings are evaluated in terms of performance at the Ar emission line both at near normal and away from normal incidence. The dependence of coating reflectance with the incidence medium, either vacuum or LAr, is considered. Some preliminary thermal tests of these coatings placed at cryogenic temperatures are also presented.

2024 JINST 19 C05028

2 Expected performance of FUV coatings for TPC

Two sorts of coatings were evaluated: narrowband multilayer (ML) coatings and broadband mirrors. Let us start with narrowband mirrors.

A potentially interesting feature for the new generation of Ar and Xe detectors is wavelength selectivity, which would allow to reject scintillation from other materials, Cherenkov radiation or to exploit the spectral richness of their scintillation. Such selectivity can be implemented in an easy way developing ML coatings tuned to specifically reflect at a wavelength of interest and to transmit at longer wavelengths (which could be handled by further optics and detectors). This was selected as the main requirement for ML coatings. The best candidate for such FUV coatings consist in MLs alternating layers of a high refractive index (n) material, typically LaF_3, with layers with a low n, typically AlF_3 or MgF_2 [24].

Photons generated by the scintillation of the Ar_2 inside the LAr TPC can impinge onto the ML from any direction. This is a challenge for narrowband coatings, which, for a ML designed at a given wavelength and incidence angle, reflectance decays away from the design angle.

For a ML tuned at normal incidence, as the incidence angle diverts from normal incidence, the band naturally shifts to shorter wavelengths. Figure 1 plots the calculated reflectance and transmittance of an $(AlF_3/LaF_3)_6$ (the subindex outside the parentheses represents the number of bilayers) ML immersed either in vacuum or in LAr for various angles of incidence. Reflectance and transmittance calculations in this research were performed with XOP-IMD software [25]. The incidence medium was taken into account in the ML optimization. As predicted, the band shifts with the incidence angle and the peak reflectance decreases. This decrease is more pronounced when the coating is immersed in LAr compared to vacuum, which limits the efficiency of the coating to an aperture from 0° to ~60° in vacuum to 0°- ~40° in LAr. The reflectance reduction when the light incidence medium switches from vacuum to LAr is attributed to the smaller n contrast of the coating materials with LAr [26] compared to such contrast with vacuum. Figure 1 also plots MLs transmittance, which evidences that these coatings are naturally transparent to longer wavelengths, not only in the longer FUV, but all the way to the infrared.

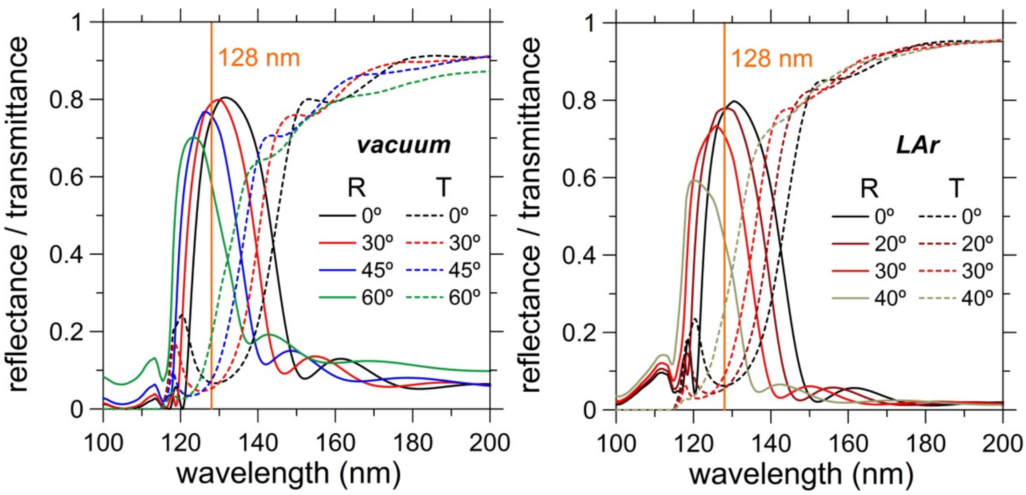

Figure 1. Calculated reflectance and transmittance as a function of wavelength for an $(AlF_3/LaF_3)_6$ ML coating aimed to reflect at 128 nm and to transmit at longer wavelengths. Calculations consider various incidence angles and the ML immersed in vacuum (left) or LAr (right).

Let us now evaluate the expected performance of a broadband mirror for photon collection at 128 nm. It consists on a reflective Al film protected with a thin MgF_2 layer. Figure 2 shows the calculated reflectance of a MgF_2-protected Al mirror. The MgF_2 layer thickness was optimized for largest average omnidirectional reflectance for the mirror immersed both in vacuum or in LAr. The optimal MgF_2 layer thickness was evaluated in terms of the maximal integrated reflectance over 2π sr, and it was found to be 27 nm for the coating in vacuum, whereas for a coating immersed in LAr the angle integrated reflectance continuously grows with decreasing MgF_2 layer thickness; since Al needs to be protected to avoid its oxidation, a minimum MgF_2 thickness with capacity to protect Al of 15 nm was considered. Contrary to the narrowband ML, the reflectance dependence of an MgF_2-protected Al mirror on the incidence angle is relatively small. For LAr-immersed mirrors, the average angular reflectance is calculated to be even larger than for the coating in vacuum. This behavior of Al/MgF_2 mirrors is positive for their use in LAr TPCs and more studies are being performed to compare their performance with the total coverage of the inner detector walls with a wavelength shifter. Additionally, these mirrors are also efficient to reflect radiation at longer wavelengths, from the FUV to the infrared and beyond.

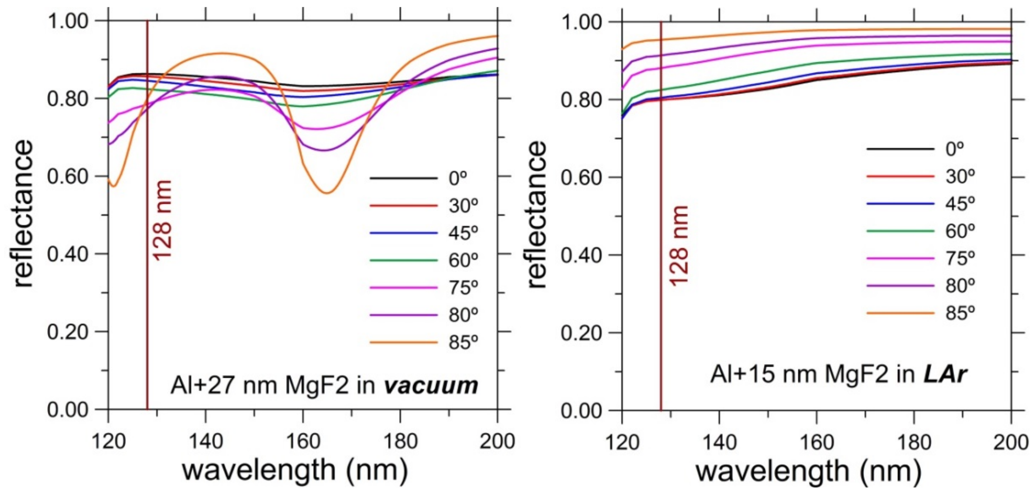

Figure 2. Calculated reflectance at various incidence angles of a MgF_2-protected Al mirror optimized for largest reflectance at 128 nm for the coating immersed either in vacuum (left) or LAr (right).

The positive behavior of the Al/MgF_2 coating in reflectance contrasts with its opacity at any spectral range from FUV to the infrared (compared to the transparency at longer wavelengths of the narrowband mirrors), due to the strong absorption of the Al film. The current performance is still moderate compared to that of Enhanced Specular Reflectors and other solutions used in the optical and UV band, but the overall performance accounting for wavelength shifting efficiency and photon detection efficiency must be evaluated coherently. This study is foreseen in a small characterization setup filled with LAr.

3 Experimental performance over cooling tests

Some preliminary cooling tests were made, which consisted in cooling down a coated substrate at temperatures close to LAr. Three samples, which were not specifically prepared for this research but had close performance to the target application, were used: two narrowband MLs [$(MgF_2/LaF_3)_{20}$ and $(MgF_2/LaF_3)_9$ deposited on CaF_2] and a 25-nm thick MgF_2-protected Al mirror deposited on glass.

2024 JINST 19 C05028

Coatings tuned at 128 nm have to survive and keep sufficient performance at the LAr temperature of −186°C (coatings tuned at ~170 nm would operate under a less cold temperature of −108°C). A thermal range of more than 200 K might originate thermal stress and hence crack generation, especially for fluoride MLs. This is due to the relatively large coefficient of thermal expansion (CTE) of the fluoride materials, particularly when compared with most used substrates, such as fused silica. Table 1 plots CTE of usual substrates and main FUV coating materials. The deleterious effect of stress increases with total coating thickness; that is why a modest number of only 6 bilayers was used in the above calculations.

The coatings used in these cryo tests had been deposited using thermal evaporation in a high-vacuum chamber. The samples had been stored in a desiccator since deposition prior to the present cooling tests. Coating FUV reflectance was measured in GOLD's reflectometer [27] (GOLD is the Spanish acronym for Thin Films Optics Group, Madrid, Spain). Details on the deposition process and the reflectometer are explained in previous publications [28–30]. Liquid N_2 (LN_2, −200°C) was used for the cryo-tests.

Table 1. The coefficient of thermal expansion (CTE) of usual substrates and FUV coating materials. Data available in [31] and references therein.

Material	**CTE ($\times 10^{-6}$/°C)**	
Substrate:		
fused silica	0.55	
CaF_2	18.85	
Coating:		
AlF_3	6.7	
MgF_2	8.5 (⊥)	13.6 (‖)
LaF_3	17 (⊥)	11 (‖)

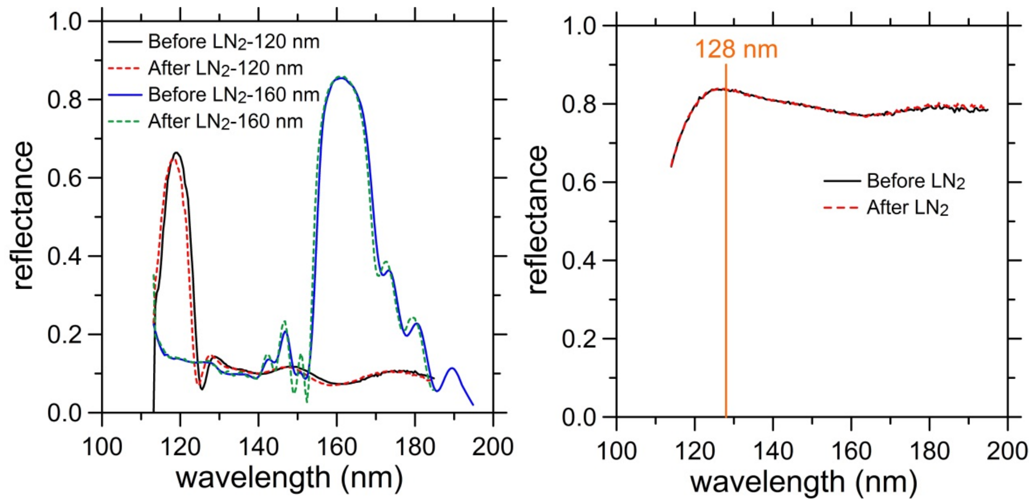

Figure 3. Reflectance as a function of wavelength for $(MgF_2/LaF_3)_9$ and $(MgF_2/LaF_3)_{20}$ MLs tuned, respectively, at 120 nm, close to the 127-nm Ar_2 line, and at 160 nm, close to the ~175-nm Xe_2 line (left) and of a 25-nm thick MgF_2-protected Al mirror optimized for largest reflectance at ~122 nm (right) both before and after immersion in LN_2. The small variation of the coating tuned at 120 nm is attributed to measuring at a different spot in the sample with some lateral gradient more than to a temperature effect.

2024 JINST 19 C05028

FUV reflectance was measured both before and after the sample was submerged in LN_2 for some minutes (later warmed to room temperature by blowing with dry N_2) and it is plotted in figure 3. For all three coatings no significant reflectance difference was observed. In practice, an optical coating in a TPC with LAr may have to be subject to several processes of cooling down to LAr and warming up back to room temperature. Hence further research is necessary to check if these coatings will survive a series of various such thermal cycles.

4 Summary

We have presented calculations and preliminary results of candidate mirrors to be used to improve the optical performance of LAr and LXe TPCs, which operate at ∼127 nm and ∼175 nm, respectively. Narrowband mirrors based on AlF_3/LaF_3 or MgF_2/LaF_3 ML coatings tuned at these wavelengths have a normal reflectance of 80% to 90%, which decreases by a few percent when the incidence medium is replaced from vacuum to LAr. For omnidirectional scintillation light in TPC's, the band shifts to shorter wavelengths for light incoming away from normal incidence, so that only a certain angle range of the incoming light can be effectively reflected by a given narrowband coating. For an optics immersed in LAr, the angle range that is efficiently reflected is narrower than for vacuum-immersed coatings, and it is limited to the ∼0°–40° range. In contrast, these coatings are naturally transparent at longer wavelengths, which can be useful in the case that distinctive spectral features are identified for the electroluminiscence process or for different ionizing radiation sources.

Broadband mirrors based on MgF_2-protected Al have normal-incidence reflectance of ∼80%. To operate in LAr, a 15-nm thick MgF_2 layer was considered to protect the Al layer and reflect the omnidirectional incoming radiation with an average reflectance >80%. These coatings not only effectively reflect the FUV, but extend their reflectance to the infrared and beyond.

We have programmed experimental studies of the performance of these mirrors and their actual effect in overall light collection efficiency in small experimental setups filled with LAr.

The two sorts of mirrors were subjected to a single cooling down process to LN_2 temperature, with no significant change in reflectance after warming up at room temperature. This is a positive result, although further tests on mirrors subjected to several cooling/warming thermal cycles would be required to confirm the stability of the coatings at cryo temperatures.

Acknowledgments

We acknowledge funding to Grant PDC2022-133788-I00 (MCIN/AEI/10.13039/501100011033, European Union NextGenerationEU/PRTR), Grant PID2019-105156GB-I00 (MCIN/AEI/10.13039/501100011033), Grant PID2019-109374GB-I00 and the "Atraccion de Talento" grant 2018-T2/TIC-10494.

References

[1] J.H. Oort, *The force exerted by the stellar system in the direction perpendicular to the galactic plane and some related problems*, *Bull. Astron. Inst. Netherlands* **6** (1932) 249.

[2] F. Zwicky, *Die Rotverschiebung von extragalaktischen Nebeln*, *Helv. Phys. Acta* **6** (1933) 110.

[3] F. Zwicky, *On the Masses of Nebulae and of Clusters of Nebulae*, *Astrophys. J.* **86** (1937) 217.

[4] Planck collaboration, *Planck 2018 results. I. Overview and the cosmological legacy of Planck*, *Astron. Astrophys.* **641** (2020) A1 [arXiv:1807.06205].

[5] S.M. Faber and J.S. Gallagher, *Masses and mass-to-light ratios of galaxies*, *Ann. Rev. Astron. Astrophys.* **17** (1979) 135.

[6] D. Clowe et al., *A direct empirical proof of the existence of dark matter*, *Astrophys. J. Lett.* **648** (2006) L109 [astro-ph/0608407].

[7] WMAP collaboration, *First year Wilkinson Microwave Anisotropy Probe (WMAP) observations: Determination of cosmological parameters*, *Astrophys. J. Suppl.* **148** (2003) 175 [astro-ph/0302209].

[8] DarkSide-20k collaboration, *DarkSide-20k: A 20 tonne two-phase LAr TPC for direct dark matter detection at LNGS*, *Eur. Phys. J. Plus* **133** (2018) 131 [arXiv:1707.08145].

[9] LZ collaboration, *First Dark Matter Search Results from the LUX-ZEPLIN (LZ) Experiment*, *Phys. Rev. Lett.* **131** (2023) 041002 [arXiv:2207.03764].

[10] XENON collaboration, *First Dark Matter Search with Nuclear Recoils from the XENONnT Experiment*, *Phys. Rev. Lett.* **131** (2023) 041003 [arXiv:2303.14729].

[11] AMS collaboration, *Towards Understanding the Origin of Cosmic-Ray Positrons*, *Phys. Rev. Lett.* **122** (2019) 041102.

[12] D. Hooper and T. Linden, *On The Origin Of The Gamma Rays From The Galactic Center*, *Phys. Rev. D* **84** (2011) 123005 [arXiv:1110.0006].

[13] D. Hooper and T. Linden, *The Gamma-Ray Pulsar Population of Globular Clusters: Implications for the GeV Excess*, *JCAP* **08** (2016) 018 [arXiv:1606.09250].

[14] CMS collaboration, *Measurement of the inclusive and differential Higgs boson production cross sections in the decay mode to a pair of τ leptons in pp collisions at $\sqrt{s} = 13$ TeV*, *Phys. Rev. Lett.* **128** (2022) 081805 [arXiv:2107.11486].

[15] ATLAS collaboration, *Performance of missing transverse momentum reconstruction with the ATLAS detector using proton-proton collisions at $\sqrt{s} = 13$ TeV*, *Eur. Phys. J. C* **78** (2018) 903 [arXiv:1802.08168].

[16] R. Santorelli et al., *Spectroscopic analysis of the gaseous argon scintillation with a wavelength sensitive particle detector*, *Eur. Phys. J. C* **81** (2021) 622 [arXiv:2012.08262].

[17] C.D.R. Azevedo et al., *Microscopic simulation of xenon-based optical TPCs in the presence of molecular additives*, *Nucl. Instrum. Meth. A* **877** (2018) 157 [arXiv:1705.09481].

[18] T. Heindl et al., *The scintillation of liquid argon*, *EPL* **91** (2010) 62002 [arXiv:1511.07718].

[19] M. Suzuki and S. Kubota, *Mechanism of proportional scintillation in argon, krypton and xenon*, *Nucl. Instrum. Meth.* **164** (1979) 197.

[20] ArDM collaboration, *ArDM: a ton-scale LAr detector for direct Dark Matter searches*, *J. Phys. Conf. Ser.* **308** (2011) 012006 [arXiv:1012.5967].

[21] A.M.F. Trindade et al., *Study of the loss of Xenon Scintillation in Xenon-Trimethylamine Mixtures*, *Nucl. Instrum. Meth. A* **905** (2018) 22 [arXiv:1812.05521].

[22] M. Piotter et al., *First time-resolved measurement of infrared scintillation light in gaseous xenon*, *Eur. Phys. J. C* **83** (2023) 482 [arXiv:2303.09344].

[23] S. Leardini et al., *Time and band-resolved scintillation in time projection chambers based on gaseous xenon*, *Eur. Phys. J. C* **82** (2022) 425 [arXiv:2112.04750].

2024 JINST 19 C05028

[24] R. Thielsch, *Optical Interference Coatings*, N. Kaiser and H.K. Pulker eds., Springer Berlin Heidelberg (2003) [DOI:10.1007/978-3-540-36386-6].

[25] D.L. Windt, *IMD — Software for modeling the optical properties of multilayer films*, Comput. Phys. **12** (1998) 360.

[26] E. Grace and J.A. Nikkel, *Index of refraction, Rayleigh scattering length, and Sellmeier coefficients in solid and liquid argon and xenon*, Nucl. Instrum. Meth. A **867** (2017) 204 [arXiv:1502.04213].

[27] GOLD Laboratory, https://gold.io.csic.es/.

[28] P. López-Reyes et al., *Optimization of the deposition parameters of MgF_2/LaF_3 narrowband reflective FUV multilayers*, Opt. Mater. Express **11** (2021) 1678.

[29] P. López-Reyes et al., *Far-UV reflectance and stress of narrowband AlF_3/LaF_3 multilayers*, Opt. Mater. Express **12** (2022) 489.

[30] P. López-Reyes et al., *Far UV narrowband mirrors tuned at H Lyman α*, Opt. Express **31** (2023) 15392.

[31] P. López-Reyes, *Narrowband mirrors based on fluorides for far UV space instrumentation*, Doctoral dissertation, Universidad Complutense de Madrid (2023).